2015 IEEE/SICE International Symposium on System Integration (SII)
December 11-13, 2015. Meijo University, Nagoya, Japan

Iterative Calculation Method for Constraint Motion by Extended Newton-Euler Method and Application for Forward Dynamics

Xiang Li, Jumpei Nishiguchi, Mamoru Minami, Takayuki Matsuno and Akira Yanou

Abstract— **There are two principal methods to derivate motion of equation of robot manipulator, which are Newton-Euler (NE) method and Lagrange method. The NE method enables to make a dynamical model of robots and it is possible to calculate internal force and torque not generating real motion of robot manipulator, seemed to be an advantage of the NE method that Lagrange method does not have. This merit can be applicable for propagations of constraint and impact force/torque when discussing humanoids walking based on strict dynamical models. So far, the NE method has been applied to a robot of open-loop serial-linkage structure. However, the NE method has been limited to a motion without contacting with environment. Although robot task to the hand contact with environment, for example assembly task, grinding task is important, it has not been formulated in the way of the NE method. So, this paper proposes iterative calculation method for representing constraint dynamical motion of robot manipulator utilizing inverse dynamic calculation the NE method, leading and enabling the forward dynamics calculation of constraint motions to be dealt recursively through proposed the extended NE method for constraint motions, with no use of explicit representation of equation of motions. We applied this method to 2-linkage and 3-linkage manipulators and evaluated its validity by numerical simulations.**

I. INTRODUCTION

There are two principal methods to derivate equation of motion of robot manipulator, which are Newton-Euler (NE) method and Lagrange method [1]. The NE method has been applied to an open-chain tree structure like a satellite [2], and biological structure such as a human body [3], but it was difficult to be used in real-time because of the large amount of computation. To reduce the amount of computation, Walker and Orin reformulated in 1980, a method of forward dynamics problem by using the NE method and its effectiveness in 1982 [4]. After that, the NE method has been widely applied such as models of non-rigid manipulator [5]. the NE method has some advantage which Lagrange method does not have, such as it can calculate internal forces and internal torque that does not produce the actual motion of the robot. This merit can be applied for force/torque propagation originated by constraint force/torque and even for impact force exerted to foot from ground when humanoid walks.

The conventional method of the NE could be limited to be applied to a robot having an open loop serial linkage structure, but the motion of hand was limited to motions without contacting external world. The NE method has been formulated for a manipulator that does not contact to the environment. Then the proposed Extend NE method in this paper is formulated to derive a equation of motion under a premise that it contacts with the environment when the robot was tasked with some grinding work or assembling work.

The problem of solving the dynamics of robot in contact with constraint, meaning the external environment has been described [6]. Therein the constraint force can be calculated by the iterative method, and it shows a problem which named the Linear Complementarity Problem (LCP) [7] that when the number of iterations is small, the residual error will occur. Also, the Articulated-Body Algorithm (ABA) [8] shows that it cannot be applied to a constraint motion, limited to the open linkage structure that the joint constraint is exactly satisfied. For this point, the extended NE method proposed in this paper is in the same direction as the researches of [8][9], in terms of that the constraints are strictly satisfied. We have devised how to combine constraint force with the iterative calculation of the NE method, by referring the method Hemami [10] has proposed. Then we propose a method for applying the inverse dynamics calculation of the extended NE method to the forward dynamics problem. And it has a characteristic different from the conventional method as a force acting on the contact portion from the external environment, not only a constraint force is discussed conventionally, a frictional force exerting contacting point is also formulated.

II. THE INVERSE DYNAMICS SOLUTION BY NEWTON-EULER METHOD DURING RESTRAINED MOTION

Here, we consider the inverse dynamics solution of constrained motion of a tip link of straight chain link manipulator which constituted by undeformed rigid links while it is contacting the undeformed environment. Considering the manipulator with n rigid links shown in Fig.1, which has a straight chain link structure and n degrees of freedom, and affected by friction force f_t and constraint force f_n exerted to hand from the ground. We will derive the equation of motion based on a coordinate system Σ_i fixed to the link i. Σ_0 is a work coordinate system fixed to the floor. The constraint condition can be defined as Eq.(1) when the hand is restrained to a restraint surface, and the $\boldsymbol{r}(\boldsymbol{q})$ is the position vector of the hand, and $\boldsymbol{q}$ is joint angle vector.

$$C(\boldsymbol{r}(\boldsymbol{q})) = 0 \tag{1}$$

Here, we can assume that $C(\boldsymbol{r}(\boldsymbol{q}))$ is differentiable respecting to $\boldsymbol{r}$, $\boldsymbol{q}$ and time t. In Fig.1, which is depicted on

X. Li, N. Jumpei, M. Minami, T. Matsuno and A. Yanou are with Graduate School of Natural Science and Technology, Okayama University, Okayama, Japan 700-8530
{pzkm87r2,en420980}@s.okayama-u.ac.jp,
{minami-m,matsuno,yanou-a}@cc.okayama-u.ac.jp

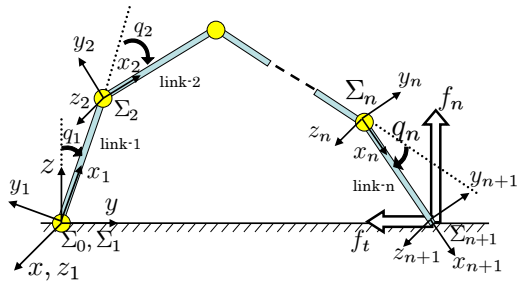

Fig. 1. n-link manipulator whose hand position is constraint by non elastic environment, which is a floor in this figure

the assumption that the robot is in contact with a floor environment, but the following discussions are not limited to discussions about the floor constraint.

First, as a forward dynamics computation of the Newton-Euler method, we can calculate the joint angular velocity ${}^i\boldsymbol{\omega}_i$ of link i toward the tip link from the root link, the joint angular acceleration ${}^i\dot{\boldsymbol{\omega}}_i$, the translational acceleration at the origin of Σ_i, ${}^i\ddot{\boldsymbol{p}}_i$, and the translational acceleration in the center of mass by the following equation. The upper left subscript shows the reference coordinate system, the lower right subscript shows the target link.

$$
\begin{aligned}
{}^i\boldsymbol{\omega}_i &= {}^{i-1}\boldsymbol{R}_i^{\mathrm{T}}\ {}^{i-1}\boldsymbol{\omega}_{i-1} + {}^i\boldsymbol{z}_i\dot{q}_i && (2)\\
{}^i\dot{\boldsymbol{\omega}}_i &= {}^{i-1}\boldsymbol{R}_i^{\mathrm{T}}\ {}^{i-1}\dot{\boldsymbol{\omega}}_{i-1} + {}^i\boldsymbol{z}_i\ddot{q}_i + {}^i\boldsymbol{\omega}_i \times ({}^i\boldsymbol{z}_i\dot{q}_i) && (3)\\
{}^i\ddot{\boldsymbol{p}}_i &= {}^{i-1}\boldsymbol{R}_i^{\mathrm{T}}\Big\{{}^{i-1}\ddot{\boldsymbol{p}}_{i-1} + {}^{i-1}\dot{\boldsymbol{\omega}}_{i-1} \times {}^{i-1}\hat{\boldsymbol{p}}_i \\
&\qquad + {}^{i-1}\boldsymbol{\omega}_{i-1} \times ({}^{i-1}\boldsymbol{\omega}_{i-1} \times {}^{i-1}\hat{\boldsymbol{p}}_i)\Big\} && (4)\\
{}^i\ddot{\boldsymbol{s}}_i &= {}^i\ddot{\boldsymbol{p}}_i + {}^i\dot{\boldsymbol{\omega}}_i \times {}^i\hat{\boldsymbol{s}}_i + {}^i\boldsymbol{\omega}_i \times ({}^i\boldsymbol{\omega}_i \times {}^i\hat{\boldsymbol{s}}_i) && (5)
\end{aligned}
$$

${}^{i-1}\boldsymbol{R}_i$ is a rotation matrix from Σ_{i-1} to Σ_i, and ${}^i\boldsymbol{z}_i = [0,0,1]^{\mathrm{T}}$ is a unit vector of rotation axis of the link i, ${}^{i-1}\hat{\boldsymbol{p}}_i$ is a position vector from the origin point of Σ_{i-1} to Σ_i, ${}^i\hat{\boldsymbol{s}}_i$ is a position vector from the origin point of Σ_i to the center of mass of link i. As the initial value, we set ${}^0\boldsymbol{\omega}_0 = \boldsymbol{0}$, ${}^0\dot{\boldsymbol{\omega}}_0 = \boldsymbol{0}$, ${}^0\ddot{\boldsymbol{p}}_0 = [0,0,g]^{\mathrm{T}}$, ${}^0\ddot{\boldsymbol{s}}_0 = \boldsymbol{0}$. Here g is the gravity acceleration.

Then, based on the inverse dynamics calculation, the Newton equation and the Euler equation of link i are derived recursively from bottom link to top link as Eq.(6)$\sim$Eq.(8).

$$
{}^{n+1}\boldsymbol{f}_{n+1} = -{}^0\boldsymbol{R}_{n+1}^{\mathrm{T}}\left\{\frac{\left(\frac{\partial C}{\partial \boldsymbol{r}}\right)}{\left\|\frac{\partial C}{\partial \boldsymbol{r}}\right\|}f_n - \frac{\dot{\boldsymbol{r}}}{\|\dot{\boldsymbol{r}}\|}f_t\right\} \qquad (6)
$$

$$
{}^i\boldsymbol{f}_i = {}^i\boldsymbol{R}_{i+1}\,{}^{i+1}\boldsymbol{f}_{i+1} + m_i\,{}^i\ddot{\boldsymbol{s}}_i \qquad (7)
$$

$$
\begin{aligned}
{}^i\boldsymbol{n}_i = {}&{}^i\boldsymbol{R}_{i+1}\,{}^{i+1}\boldsymbol{n}_{i+1} + {}^i\boldsymbol{I}_i\,{}^i\dot{\boldsymbol{\omega}}_i + {}^i\boldsymbol{\omega}_i \times ({}^i\boldsymbol{I}_i\,{}^i\boldsymbol{\omega}_i)\\
&+ {}^i\hat{\boldsymbol{s}}_i \times (m_i\,{}^i\ddot{\boldsymbol{s}}_i) + {}^i\hat{\boldsymbol{p}}_{i+1} \times ({}^i\boldsymbol{R}_{i+1}\,{}^{i+1}\boldsymbol{f}_{i+1}) \qquad (8)
\end{aligned}
$$

The ${}^i\boldsymbol{f}_i$, ${}^i\boldsymbol{n}_i$ in Σ_i show the force and moment exerted on link i from link $(i+1)$. And ${}^i\boldsymbol{I}_i$ denotes the inertia matrix of the center of gravity of link i. Because ${}^{n+1}\boldsymbol{f}_{n+1}$ that is a force transmitting to top link from the floor will be the reaction force of constraint force, we can calculate it as shown in Eq.(6). About constraint motion, we discuss motions with statical and kinetic friction based on friction fundamentals, i.e. (i)The direction of f_n and the friction force f_t exerted on external contact portion are orthogonal as shown in Fig.1, (ii)f_t is determined in proportion to f_n: $f_t = Kf_n$ (K is the coefficient of friction force : $0 < K < 1$). The constraint force f_n can be determined by the method described in the next chapter. Equation of motion of all links can be obtained by repeating the Newton and Euler's equation in Eq.(7) and (8) from hand to root link. Giving the Σ_i to all joints that have rotation axes about the ${}^iz_i$-axis, the relationship between ${}^i\boldsymbol{n}_i$ and joint driving force τ_i can be calculated as follows.

$$
\tau_i = {}^i\boldsymbol{z}_i^{\mathrm{T}}\ {}^i\boldsymbol{n}_i + D_i\dot{q}_i \qquad (9)
$$

Here, D_i represents the viscous friction coefficient of joint i. The merit of the NE method applicable for the calculations of internal force/torque is explained by Eq.(6)-(8), that is ${}^i\boldsymbol{f}_i$ and ${}^i\boldsymbol{n}_i$ include f_n and f_t. The ${}^i\boldsymbol{f}_i$ and ${}^i\boldsymbol{n}_i$ include not only force/torque producing real motions as shown in Eq.(9), but also internal force/torque not effecting real motion, which may break the structure of robots. Furthermore the influence of impact force from ground to the humanoid walking can also be discussed by the above the NE method.

III. DERIVATION OF CONSTRAINT FORCE

In this chapter we describe a method of deriving the constraint force f_n. A condition of hand constraint state of manipulator robot is represented by Eq.(1), and its equation of motion is represented by Eq.(10).

$$
\boldsymbol{M}(\boldsymbol{q})\ddot{\boldsymbol{q}} + \boldsymbol{h}(\boldsymbol{q},\dot{\boldsymbol{q}}) + \boldsymbol{g}(\boldsymbol{q}) + \boldsymbol{D}\dot{\boldsymbol{q}} - (\boldsymbol{j}_c - \boldsymbol{j}_t K)f_n = \boldsymbol{\tau} \quad (10)
$$

$\boldsymbol{M}(\boldsymbol{q})$ is inertia matrix with $n \times n$, $\boldsymbol{h}(\boldsymbol{q},\dot{\boldsymbol{q}})$ and $\boldsymbol{g}(\boldsymbol{q})$ are vector with $n \times 1$ representing the term of centrifugal force/Coriolis force and the gravity term, D is a diagonal matrix $\boldsymbol{D} = diag[D_1, D_2, \cdots, D_n]$ with $n \times n$ representing the viscous friction coefficients of joints, $\boldsymbol{\tau}$ is a input torque vector with $n \times 1$, and $\boldsymbol{q} = [q_1,\ q_2,\ \cdots,\ q_n]^{\mathrm{T}}$ is the joint angle vector with $n \times 1$. Besides, $\boldsymbol{j}_c$ and $\boldsymbol{j}_t$ are defined as follows.

$$
\boldsymbol{j}_c \triangleq \left(\frac{\partial \boldsymbol{r}}{\partial \boldsymbol{q}^{\mathrm{T}}}\right)^{\mathrm{T}}\left(\frac{\partial C}{\partial \boldsymbol{r}}\right)\Big/\left\|\frac{\partial C}{\partial \boldsymbol{r}}\right\|,\quad \boldsymbol{j}_t \triangleq \left(\frac{\partial \boldsymbol{r}}{\partial \boldsymbol{q}^{\mathrm{T}}}\right)^{\mathrm{T}}\frac{\dot{\boldsymbol{r}}}{\|\dot{\boldsymbol{r}}\|} \qquad (11)
$$

Making second-order differentiation of Eq.(1) by time t to determine the constraint condition $\ddot{\boldsymbol{q}}$, we have

$$
\dot{\boldsymbol{q}}^T\left[\frac{\partial}{\partial \boldsymbol{q}}\left(\frac{\partial C}{\partial \boldsymbol{q}^T}\right)\right]\dot{\boldsymbol{q}} + \left(\frac{\partial C}{\partial \boldsymbol{q}^T}\right)\ddot{\boldsymbol{q}} = 0. \qquad (12)
$$

In order to make manipulator be always constrained to restraint surface, the solution $\boldsymbol{q}(t)$ of Eq.(10) should satisfy the Eq.(1) regardless of the time t. When $\ddot{\boldsymbol{q}}$ in Eq.(10) and $\ddot{\boldsymbol{q}}$ which is satisfied to the Eq.(12) obtained by the time derivative of Eq.(1) take the same value, the $\boldsymbol{q}(t)$ in Eq.(10) will satisfy Eq.(1). Erasing the $\dot{\boldsymbol{q}}$ by Eq.(10) and Eq.(12).

$$
\begin{aligned}
&\left(\frac{\partial C}{\partial \boldsymbol{q}^{\mathrm{T}}}\right)\boldsymbol{M}^{-1}\left(\frac{\partial C}{\partial \boldsymbol{q}^{\mathrm{T}}}\right)^{\mathrm{T}}\frac{f_n}{\left\|\frac{\partial C}{\partial \boldsymbol{r}^{\mathrm{T}}}\right\|}\\
&= \left(\frac{\partial C}{\partial \boldsymbol{q}^{\mathrm{T}}}\right)\boldsymbol{M}^{-1}(\boldsymbol{j}_t K f_n + \boldsymbol{D}\dot{\boldsymbol{q}} + \boldsymbol{h} + \boldsymbol{g} - \boldsymbol{\tau})\\
&-\dot{\boldsymbol{q}}^{\mathrm{T}}\left[\frac{\partial}{\partial \boldsymbol{q}}\left(\frac{\partial C}{\partial \boldsymbol{q}^{\mathrm{T}}}\right)\right]\dot{\boldsymbol{q}} \qquad (13)
\end{aligned}
$$

We got Eq.(13). Here, we define m_c as follow.

$$m_c \triangleq (\partial C/\partial \boldsymbol{q}^{\mathrm{T}})\boldsymbol{M}^{-1}(\partial C/\partial \boldsymbol{q}^{\mathrm{T}})^{\mathrm{T}} \tag{14}$$

$\boldsymbol{M}^{-1}$ is nonsingular, $\partial C/\partial \boldsymbol{q}^{\mathrm{T}} = (\partial C/\partial \boldsymbol{r}^{\mathrm{T}})(\partial \boldsymbol{r}/\partial \boldsymbol{q}^{\mathrm{T}})$, C is a curved surface to satisfy the $\partial C/\partial \boldsymbol{r}^{\mathrm{T}} \neq \boldsymbol{0}$. Here, assuming the $\partial \boldsymbol{r}/\partial \boldsymbol{q}^{\mathrm{T}}$ is full row rank, and to be considered with the exception of singular configuration, there will be $m_c \neq 0$, since $\partial C/\partial \boldsymbol{q}^{\mathrm{T}} \neq \boldsymbol{0}$. By using m_c, Eq.(13) can be rewritten as Eq.(15).

$$\begin{aligned} m_c f_n = \left\| \frac{\partial C}{\partial \boldsymbol{r}^{\mathrm{T}}} \right\| \Big\{ \left(\frac{\partial C}{\partial \boldsymbol{q}^{\mathrm{T}}} \right) \boldsymbol{M}^{-1} (\boldsymbol{j}_t K f_n + \boldsymbol{D}\dot{\boldsymbol{q}} \\ + \boldsymbol{h} + \boldsymbol{g} - \boldsymbol{\tau}) - \dot{\boldsymbol{q}}^{\mathrm{T}} \left[\frac{\partial}{\partial \boldsymbol{q}} \left(\frac{\partial C}{\partial \boldsymbol{q}^{\mathrm{T}}} \right) \right] \dot{\boldsymbol{q}} \Big\} \end{aligned} \tag{15}$$

Here, we define $\boldsymbol{d}^{\mathrm{T}}$ as follow.

$$\boldsymbol{d}^{\mathrm{T}} \triangleq \left\| \frac{\partial C}{\partial \boldsymbol{r}^{\mathrm{T}}} \right\| \left(\frac{\partial C}{\partial \boldsymbol{q}^{\mathrm{T}}} \right) \boldsymbol{M}^{-1} \tag{16}$$

So, Eq.(15) can be rewritten as follow.

$$\begin{aligned} m_c f_n = \boldsymbol{d}^{\mathrm{T}} \boldsymbol{j}_t K f_n - \boldsymbol{d}^{\mathrm{T}} \boldsymbol{\tau} + \boldsymbol{d}^{\mathrm{T}} \{\boldsymbol{D}\dot{\boldsymbol{q}} + \boldsymbol{h} + \boldsymbol{g}\} \\ - \left\| \frac{\partial C}{\partial \boldsymbol{r}^{\mathrm{T}}} \right\| \dot{\boldsymbol{q}}^{\mathrm{T}} \left[\frac{\partial}{\partial \boldsymbol{q}} \left(\frac{\partial C}{\partial \boldsymbol{q}^{\mathrm{T}}} \right) \right] \dot{\boldsymbol{q}} \end{aligned} \tag{17}$$

Here, we define a as follow.

$$a \triangleq \boldsymbol{d}^{\mathrm{T}} \{\boldsymbol{D}\dot{\boldsymbol{q}} + \boldsymbol{h} + \boldsymbol{g}\} - \left\| \frac{\partial C}{\partial \boldsymbol{r}^{\mathrm{T}}} \right\| \dot{\boldsymbol{q}}^{\mathrm{T}} \left[\frac{\partial}{\partial \boldsymbol{q}} \left(\frac{\partial C}{\partial \boldsymbol{q}^{\mathrm{T}}} \right) \right] \dot{\boldsymbol{q}} \tag{18}$$

We will get Eq.(19).

$$m_c f_n = \boldsymbol{d}^{\mathrm{T}} \boldsymbol{j}_t K f_n - \boldsymbol{d}^{\mathrm{T}} \boldsymbol{\tau} + a \tag{19}$$

We define A as follow.

$$A \triangleq m_c - \boldsymbol{d}^{\mathrm{T}} \boldsymbol{j}_t K \tag{20}$$

We can get Eq.(21).

$$A f_n = a - \boldsymbol{d}^{\mathrm{T}} \boldsymbol{\tau} \tag{21}$$

Constraint force f_n of constraint point can be determined by the algebraic equation of the input torque $\boldsymbol{\tau}$ when $A \neq 0$.

A. Differentiation of Jacobian Matrix

By deforming the second term in the right side of Eq.(18), we can obtain Eq.(22). Here we put the $(\partial \boldsymbol{r}/\partial \boldsymbol{q}^{\mathrm{T}}) = \boldsymbol{J}_p$ that is the Jacobian matrix for the $\boldsymbol{q}$ against the hand position $\boldsymbol{r}$.

$$\begin{aligned} & \dot{\boldsymbol{q}}^{\mathrm{T}} \left[\frac{\partial}{\partial \boldsymbol{q}} \left(\frac{\partial C}{\partial \boldsymbol{q}^{\mathrm{T}}} \right) \right] \dot{\boldsymbol{q}} \\ &= \frac{d\boldsymbol{q}^{\mathrm{T}}}{dt} \left[\frac{\partial}{\partial \boldsymbol{q}} \left(\frac{\partial C}{\partial \boldsymbol{r}^{\mathrm{T}}} \frac{\partial \boldsymbol{r}}{\partial \boldsymbol{q}^{\mathrm{T}}} \right) \right] \dot{\boldsymbol{q}} \\ &= \frac{d}{dt} \left(\frac{\partial C}{\partial \boldsymbol{r}^{\mathrm{T}}} \boldsymbol{J}_p \right) \dot{\boldsymbol{q}} \\ &= \left[\frac{d}{dt} \left(\frac{\partial C}{\partial \boldsymbol{r}^{\mathrm{T}}} \right) \boldsymbol{J}_p + \frac{\partial C}{\partial \boldsymbol{r}^{\mathrm{T}}} \frac{d\boldsymbol{J}_p}{dt} \right] \dot{\boldsymbol{q}} \end{aligned} \tag{22}$$

Therefore, it is necessary to obtain the time derivative of the Jacobian matrix to determine the a of Eq.(18), following is a calculation method of $\dot{\boldsymbol{J}}_p(\boldsymbol{q})$.

First, assuming that the robot is constituted by only the rotational joint, the Jacobian matrix $\boldsymbol{J}_i$ of the i-th link can be derived as follow.

$$\begin{aligned} \boldsymbol{J}_i &= \begin{bmatrix} {}^0\boldsymbol{z}_1 \times {}^0\boldsymbol{p}_{i,1} & {}^0\boldsymbol{z}_2 \times {}^0\boldsymbol{p}_{i,2} & \cdots & {}^0\boldsymbol{z}_n \times {}^0\boldsymbol{p}_{i,n} \\ {}^0\boldsymbol{z}_1 & {}^0\boldsymbol{z}_2 & \cdots & {}^0\boldsymbol{z}_n \end{bmatrix} \\ &= \begin{bmatrix} \boldsymbol{J}_{pi} \\ \boldsymbol{J}_{ri} \end{bmatrix} \quad (i = 1, 2, \cdots, n+1) \end{aligned} \tag{23}$$

Here, the $\boldsymbol{J}_{pi}$ and J_{ri} represent position and orientation Jacobian matrix of configuration of the link i, ${}^0\boldsymbol{p}_i$ is a position vector of i-th link from root link, ${}^0\boldsymbol{p}_{n+1}$ is a position vector of hand from the root of manipulator. And ${}^0\boldsymbol{z}_i$, ${}^0\boldsymbol{p}_{n+1,i}$ are defined as follows.

$${}^0\boldsymbol{z}_i = {}^0\boldsymbol{R}_i{}^i\boldsymbol{z}_i \tag{24}$$

$${}^i\boldsymbol{z}_i = [0, 0, 1]^{\mathrm{T}} \tag{25}$$

$${}^0\boldsymbol{p}_{n+1,i} = {}^0\boldsymbol{p}_{n+1} - {}^0\boldsymbol{p}_i \tag{26}$$

The following equation can be obtained by differentiating the both of Eq.(24) and Eq.(26) by time t.

$${}^0\dot{\boldsymbol{z}}_i = {}^0\dot{\boldsymbol{R}}_i{}^i\boldsymbol{z}_i + {}^0\boldsymbol{R}_i{}^i\dot{\boldsymbol{z}}_i = {}^0\dot{\boldsymbol{R}}_i{}^i\boldsymbol{z}_i = {}^0\boldsymbol{\omega}_i \times {}^0\boldsymbol{R}_i{}^i\boldsymbol{z}_i \tag{27}$$

$${}^0\dot{\boldsymbol{p}}_{n+1,i} = {}^0\dot{\boldsymbol{p}}_{n+1} - {}^0\dot{\boldsymbol{p}}_i = \boldsymbol{J}_{p(n+1)}\dot{\boldsymbol{q}} - \boldsymbol{J}_{pi}\dot{\boldsymbol{q}} \tag{28}$$

Then, using Eq.(27), (28), and differentiating ${}^0\boldsymbol{z}_i \times {}^0\boldsymbol{p}_{n+1,i}$ in Eq.(23) by time t, we will get Eq.(29).

$$\begin{aligned} & \frac{d\left({}^0\boldsymbol{z}_i \times {}^0\boldsymbol{p}_{n+1,i}\right)}{dt} = {}^0\dot{\boldsymbol{z}}_i \times {}^0\boldsymbol{p}_{n+1,i} + {}^0\boldsymbol{z}_i \times {}^0\dot{\boldsymbol{p}}_{n+1,i} \\ &= \left({}^0\boldsymbol{\omega}_i \times {}^0\boldsymbol{R}_i{}^i\boldsymbol{z}_i\right) \times {}^0\boldsymbol{p}_{n+1,i} \\ &+ {}^0\boldsymbol{z}_i \times \left(\boldsymbol{J}_{p(n+1)}\dot{\boldsymbol{q}} - \boldsymbol{J}_{pi}\dot{\boldsymbol{q}}\right) \end{aligned} \tag{29}$$

Therefore, the time derivative of the Jacobian matrix can be calculated by the following equation.

$$\begin{aligned} \dot{\boldsymbol{J}} = [& \begin{matrix} \left({}^0\boldsymbol{\omega}_1 \times {}^0\boldsymbol{R}_1{}^i\boldsymbol{z}_i\right) \times {}^0\boldsymbol{p}_{n+1,1} + {}^0\boldsymbol{z}_1 \times \left(\boldsymbol{J}_{p(n+1)}\dot{\boldsymbol{q}} - \boldsymbol{J}_{p1}\dot{\boldsymbol{q}}\right) \\ {}^0\boldsymbol{\omega}_1 \times {}^0\boldsymbol{R}_1{}^1\boldsymbol{z}_1 \end{matrix} \\ & \cdots \begin{matrix} \left({}^0\boldsymbol{\omega}_n \times {}^0\boldsymbol{R}_n{}^n\boldsymbol{z}_n\right) \times {}^0\boldsymbol{p}_{n+1,n} + {}^0\boldsymbol{z}_n \times \left(\boldsymbol{J}_{p(n+1)}\dot{\boldsymbol{q}} - \boldsymbol{J}_{pn}\dot{\boldsymbol{q}}\right) \\ \cdots {}^0\boldsymbol{\omega}_n \times {}^0\boldsymbol{R}_n{}^n\boldsymbol{z}_n \end{matrix}] \end{aligned} \tag{30}$$

IV. SOLUTION OF THE FORWARD DYNAMICS PROBLEM

It is not easy to calculate $\boldsymbol{M}(\boldsymbol{q})$, $\boldsymbol{h}(\boldsymbol{q}, \dot{\boldsymbol{q}})$, $\boldsymbol{g}(\boldsymbol{q})$ directly in Eq.(10) which is the equation of motion of the n links multi-joint manipulator when its n becomes larger. Following describes the solution of the forward dynamics problem by using the NE inverse dynamics solution as follows.

First, define $\boldsymbol{b} = \boldsymbol{h}(\boldsymbol{q}, \dot{\boldsymbol{q}}) + \boldsymbol{g}(\boldsymbol{q}) + \boldsymbol{D}\dot{\boldsymbol{q}}$ and $\boldsymbol{\tau}_p$ as the left-hand side of Eq.(10).

$$\boldsymbol{M}(\boldsymbol{q})\ddot{\boldsymbol{q}} + \boldsymbol{b} - (\boldsymbol{j}_c - \boldsymbol{j}_t K) f_n = \boldsymbol{\tau}_p \tag{31}$$

When the inverse dynamics calculation expresses as $\boldsymbol{\tau}_p = INV(\boldsymbol{q}, \dot{\boldsymbol{q}}, \ddot{\boldsymbol{q}}, \boldsymbol{g}, f_n, K)$ shown in Eq.(2)∼Eq.(9), the following equation can be obtained.

$$\boldsymbol{M}(\boldsymbol{q})\ddot{\boldsymbol{q}} + \boldsymbol{b} - (\boldsymbol{j}_c - \boldsymbol{j}_t K) f_n = INV(\boldsymbol{q}, \dot{\boldsymbol{q}}, \ddot{\boldsymbol{q}}, \boldsymbol{g}, f_n, K) \tag{32}$$

Here, $\boldsymbol{b} = INV(\boldsymbol{q}, \dot{\boldsymbol{q}}, \boldsymbol{0}, \boldsymbol{g}, 0, K)$ can be obtained by substituting $\ddot{\boldsymbol{q}} = \boldsymbol{0}$, $f_n = 0$ in Eq.(32), then there will be $\boldsymbol{M}_i = \boldsymbol{M}(\boldsymbol{q})\boldsymbol{e}_i = INV(\boldsymbol{q}, \boldsymbol{0}, \boldsymbol{e}_i, \boldsymbol{0}, 0, K)$ by substituting

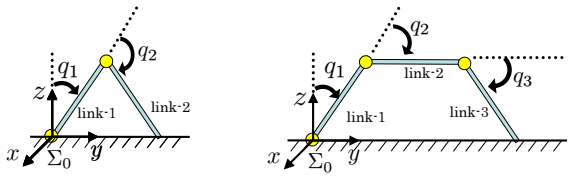

(a) 2-link manipulator (b) 3-link manipulator

Fig. 2. a) is model of 2-link manipulator (initial angle: $\boldsymbol{q} = [-\pi/6, -2\pi/3]$) and (b) is model of 3-link manipulator (initial angle: $\boldsymbol{q} = [-\pi/6, -\pi/3, -\pi/3]^{\mathrm{T}}$).

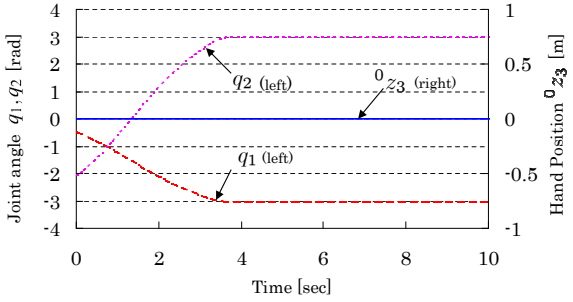

Fig. 3. Time responses of hand position ${}^0z_3$ (right scale) and joint angles q_1, q_2 (left scale) of 2-link manipulator are plotted. Input torque was set to $\boldsymbol{\tau} = [-3, 3]^{\mathrm{T}}$. This chart shows that hand position is constrainted in ${}^0z_3 = 0$ at all times by the proposed method.

$\dot{\boldsymbol{q}} = \boldsymbol{0}$, $\ddot{\boldsymbol{q}} = \boldsymbol{e}_i$, $\boldsymbol{g} = \boldsymbol{0}$, $f_n = 0$ into Eq.(32). $\boldsymbol{M}_i$ is a vector representing the i-th column of the inertia matrix, $\boldsymbol{e}_i = [0, \cdots, 1(i), 0, \cdots, 0]^{\mathrm{T}}$ is an unit vector that the i-th element with the '1', element of $\boldsymbol{M}(\boldsymbol{q})$ is calculated for each column. Besides, $\boldsymbol{j}_t$ can be obtained through $\boldsymbol{j}_c$ shown in Eq.(33) and $\boldsymbol{\tau}$ defined in Eq.(34) as shown next.

$$\boldsymbol{j}_c = INV(\boldsymbol{q}, \boldsymbol{0}, \boldsymbol{0}, \boldsymbol{0}, -1, 0) \tag{33}$$

$$\tilde{\boldsymbol{\tau}} \triangleq \boldsymbol{j}_c - \boldsymbol{j}_t = INV(\boldsymbol{q}, \boldsymbol{0}, \boldsymbol{0}, \boldsymbol{0}, -1, 1) \tag{34}$$

$$\boldsymbol{j}_t = \boldsymbol{j}_c - \tilde{\boldsymbol{\tau}} \tag{35}$$

Based on these equations and $\boldsymbol{d}^{\mathrm{T}}$, a, A that were calculated in Eq.(16), (18) and (20), we can calculate f_n in Eq.(21).

Here, we define the $\boldsymbol{b}_n = \boldsymbol{b} - (\boldsymbol{j}_c - \boldsymbol{j}_t K) f_n$, and substitute $\ddot{\boldsymbol{q}} = \boldsymbol{0}$ into $\boldsymbol{b}_n$. And by using the f_n obtained above, it is possible to obtain $\boldsymbol{b}_n = INV(\boldsymbol{q}, \dot{\boldsymbol{q}}, \boldsymbol{0}, \boldsymbol{g}, f_n, K)$. Thus, the angular acceleration $\ddot{\boldsymbol{q}}$ of each link during restrained motion is calculated as follow.

$$\ddot{\boldsymbol{q}} = \boldsymbol{M}^{-1}(\boldsymbol{\tau} - \boldsymbol{b}_n) \tag{36}$$

By using the numerical integration of $\ddot{\boldsymbol{q}}$ of the given equation, it is possible to perform the forward dynamics calculations of manipulator that the tip link is constrained and contacting with object without explicitly requiring the equation of motion in Eq.(10).

V. Numerical Simulation

In this chapter, we will confirm the constrained motion that satisfying the equation of constrained motion in Eq.(1) by the proposed method described in chapter 2∼chapter 4, using the simulation of 2-link and 3-link manipulators. These manipulator models are with small linkages, but they are suitable for checking whether the proposed algorithm is correct. The simulation environment was used by "Borland

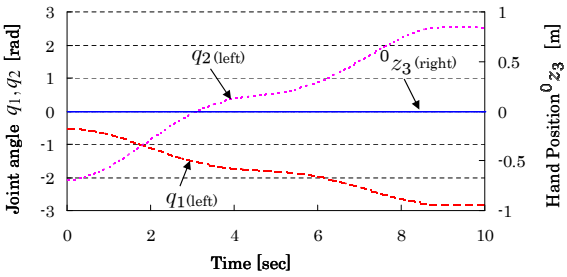

Fig. 4. Hand position and joint angles(2-link, $\boldsymbol{\tau} = [3\sin\pi t/3, 3\sin\pi t/3]^{\mathrm{T}}$)

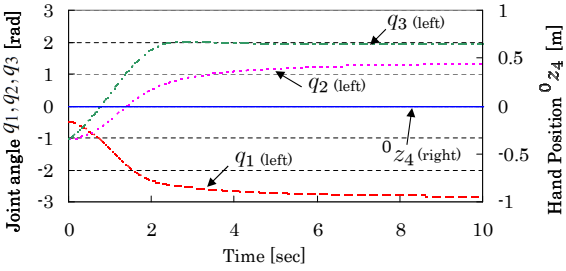

Fig. 5. Hand position and joint angles(3-link, $\boldsymbol{\tau} = [3, 3, 3]^{\mathrm{T}}$)

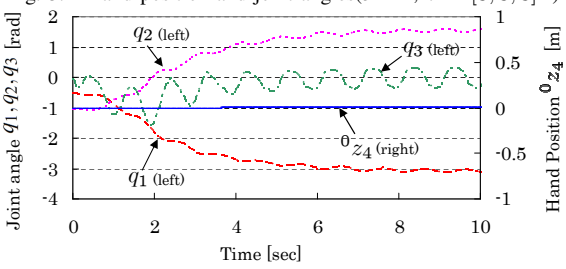

Fig. 6. Hand position and joint angles(3-link, $\boldsymbol{\tau} = [-3\cos 2\pi t, -3\sin 2\pi t, 3\cos 2\pi t]^{\mathrm{T}}$)

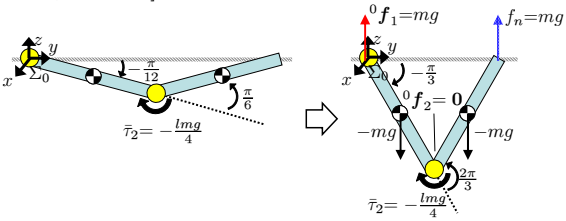

(a) (b)

Fig. 7. Initial angle is set to $\boldsymbol{q} = [-\pi/12, \pi/6]^{\mathrm{T}}$ as (a), and a input torque compensating gravity and normal force in such a way as to converge at $\boldsymbol{q} = [-\pi/3, 2\pi/3]^{\mathrm{T}}$ as (b) is set to $\bar{\boldsymbol{\tau}} = [0, -lmg/4]^{\mathrm{T}}$.

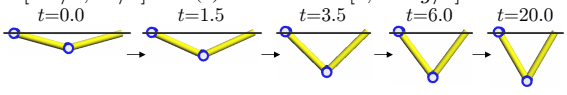

Fig. 8. Screen shot of free response of 2-link manipulator

C++ Builder Professional Ver. 5.0" for program creation, and the "Open GL Ver. 1.5.0" for display. And we set the numerical integration time of Runge-Kutta to 1.0×10^{-2} [sec], the friction coefficient of ground to $K = 0.2$ and $f_t = 0.2 f_n$.

A. Confirmation of Constraint Condition Being Kept

Figure 2 shows the simulation of restraint motion by the 2-link and 3-link manipulators. As the physical parameters, we set the mass and length of each link are $m_i = 1.0$[kg],

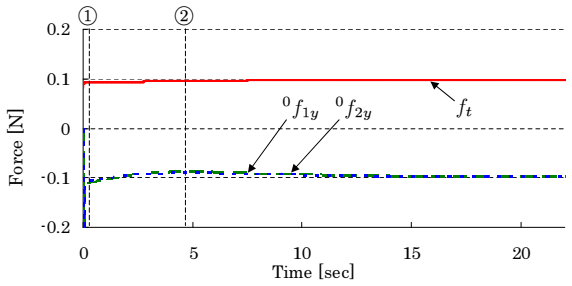

Fig. 9. Time response of y component of forces acting on each link $^0f_{1y}$, $^0f_{2y}$ and frictional force f_t of 2-link manipulator are plotted.

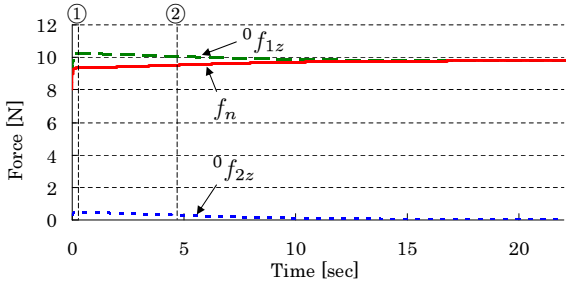

Fig. 10. Time response of z component of forces acting on each link $^0f_{1z}$, $^0f_{2z}$ and normal force f_n of 2-link manipulator are plotted.

$l_i = 0.5$[m], the viscous friction coefficient of each joint is $D_i = 3.0$[N·m·s/rad], and we set the initial position as shown in Fig.2(2-link:$\boldsymbol{q} = [-\pi/6, -2\pi/3]$,3-link:$\boldsymbol{q} = [-\pi/6, -\pi/3, -\pi/3]^{\mathrm{T}}$), this simulation was performed by varying an input torque $\boldsymbol{\tau}$ $[N]$. As shown in Fig.2, it is the motion of y-z plane in both of the 2-link and 3-link manipulators.

As an example of the arbitrary input for 2-link manipulator, when two kinds of input $\boldsymbol{\tau} = [-3, 3]^{\mathrm{T}}$, $\boldsymbol{\tau} = [3\sin\pi t/3, 3\sin\pi t/3]^{\mathrm{T}}$ are given, and the change of time of z coordinate $^0z_3$ of the tip of link 2 and the angle q_1, q_2 of each link are shown in Fig.3 and Fig.4 respectively. Similarly, when two kinds of input $\boldsymbol{\tau} = [3, 3, 3]^{\mathrm{T}}$, $\boldsymbol{\tau} = [-3\cos 2\pi t, -3\sin 2\pi t, 3\cos 2\pi t]^{\mathrm{T}}$ for 3-link manipulator are given, the change of time of z coordinate $^0z_4$ of 3rd-link's tip and the angle q_1, q_2, q_3 of each link are shown in Fig.5 and Fig.6 respectively. Because from these graphs, the coordinate $^0z_3$, $^0z_4$ of the tip link are always constrained to 0 even though $\boldsymbol{q}$ $\boldsymbol{\tau}$ are input differently, so it was confirmed that it is possible to express the constraint state by iterative calculation proposed in this paper.

TABLE I

PHYSICAL PARAMETERS OF 2-LINK MANIPULATOR

Link number i	1 (i=1)	2 (i=2)
m_i [kg]	1.0	1.0
l_i [m]	0.5	0.5
D_i [N · m · s/rad]	3.0	3.0
τ_i [N · m]	0	$-4.9/4$
g [m/s^2]	9.8	
K	0.01	

TABLE II

INITIAL AND CONVERGED VALUE OF $q_1, q_2, {}^0f_1, {}^0f_2, {}^0f_n$

Link number i	1 (i=1)	2 (i=2)
Initial angle q_i [rad]	$-7\pi/12$	$\pi/6$
Converged value of q_i [rad]	$-5\pi/6$	$2\pi/3$
Converged value of $^0\boldsymbol{f}_i$ [N]	$[0, -0.098, 9.8]^{\mathrm{T}}$	$[0, -0.098, 0]^{\mathrm{T}}$
Converged value of ^0f_n [N]	9.8	

B. Force Acting on Joints During Restraint Motion

In the previous section, the proposed method for generation of restraint motion was confirmed that the constraint dynamics expresses that the time-varying motion of tip link always satisfies the constraint condition. The calculation of force $^i\boldsymbol{f}_i$ and moment $^i\boldsymbol{n}_i$ acting on the link i from link $i-1$ are shown in Eq.(7),(8) and it is a part of the inverse dynamics calculation process of the NE method, a point of note in this subsection is that it has a feature that can calculate both of the force and torque directly producing motions and those irrelevantly connected motions of manipulator. Also, because the exerting force described by the coordinate system Σ_0 can be calculated by $^0\boldsymbol{f}_i = {}^0\boldsymbol{R}_i{}^i\boldsymbol{f}_i$, we will confirm whether the acting force $^0\boldsymbol{f}_i$ during the restraint motion is correct, and justify the time profile of the acting force and constraint force in this section.

First, we examined the acting force and constraint force acting between each link of 2-link manipulator. Constraint condition is $z = 0$, and is not $z \leq 0$. This means the space under $z = 0$ is invasive, then the shape of 2-link manipulator under $z = 0$ line is possible in the following simulations. In order to avoid that the equilibrium point of the initial configuration and target one becomes singular, we give Fig.7(a) as the initial shape, also we give $\bar{\boldsymbol{\tau}}$ as is given by Eq.(37) as an input to compensate for the gravity and constraint force that can make the position of Fig.7(b) becomes a stable equilibrium point.

$$\bar{\boldsymbol{\tau}} = [0, -mgl/4]^{\mathrm{T}} \tag{37}$$

Here we set $l_1 = l_2 = l$, coefficient of friction is $K = 0.01$, the initial position as shown in Fig.7(a) is $\boldsymbol{q} = [-7\pi/12, \pi/6]$. The simulation will not stop until the manipulator is in stationary state(it is determined as to be stationary when the angular velocity of each joint satisfies $|\dot{q}_i| < 0.001$ [rad/s]). Fig.8 shows the screen shot of the simulation, Fig.9 shows the time response of the y-component of the force $^0\boldsymbol{f}_1 = [{}^0f_{1x}, {}^0f_{1y}, {}^0f_{1z}]^{\mathrm{T}}$, $^0\boldsymbol{f}_2 = [{}^0f_{2x}, {}^0f_{2y}, {}^0f_{2z}]^{\mathrm{T}}$ acting on each joint and the frictional force f_t acting on tip link. Figure 10 shows the time profile of the z-component of the force $^0\boldsymbol{f}_1$, $^0\boldsymbol{f}_2$ and constraint force f_n, and Table 1 shows the physical parameters, and Table 2 shows the initial value and converged value for equilibrium configuration.

We set ① as the time of initial motion at $t = 0.10$, and ② as the time at $t = 4.85$ that are shown in Fig.9, 10. Noticing the time of ①, ②, Fig.11 represents the force acting on y, z directions and the direction of acceleration at those time points. As the force acting on link i, f_{iy}, f_{iz} is the y-component, z-component of the force acting on link i from link $i-1$, $-f_{(i+1)y}$, $-f_{(i+1)z}$ is the y-component,

z-component of the force acting on link i from link $i+1$, f_n is reacting force, f_t is frictional force, mg is gravity. Figure 11(a) represents the motion of hand at time① that accelerates toward y-axis minus direction, Fig.11(c) represents that the motion is decelerating in the y-axis plus direction. Although, there appears an acceleration to the falling direction(z-axis minus direction) in Fig.11(b) at time①, the direction of acceleration is z-axis plus direction at time② as in Fig.11(d), it is a deceleration motion.

Concerning force acting on link 1 and link 2, Fig.9 shows the force acting in y-direction, Fig.10 shows the force acting in z-direction. In the case of ① ($t = 0.10$), the force becomes ${}^0\boldsymbol{f}_1 = [0, -0.129, 10.252]^{\mathrm{T}}$, ${}^0\boldsymbol{f}_2 = [0, -0.120, 0.464]^{\mathrm{T}}$, $f_t = 0.093$, $f_n = 9.324$. Then the translational acceleration of the center of mass of link i based on Σ_0 by ${}^0\ddot{\boldsymbol{s}}_i = {}^0\boldsymbol{R}_i\,{}^i\ddot{\boldsymbol{s}}_i$, and Ⓐ${}^0\ddot{\boldsymbol{s}}_1 = [0, -0.009, -0.012]^{\mathrm{T}}$, ${}^0\ddot{\boldsymbol{s}}_2 = [0, -0.027, -0.012]^{\mathrm{T}}$ can be derived. Furthermore we used ${}^0\hat{\boldsymbol{f}}_i = [{}^0\hat{f}_{ix}, {}^0\hat{f}_{iy}, {}^0\hat{f}_{iz}]^{\mathrm{T}}$ to show all the external forces acting on link i at the time of $t = 0.10$, and by exam these,

$$
\begin{aligned}
{}^0\hat{f}_{1y} &= {}^0f_{1y} - {}^0f_{2y} = -0.009 && (38)\\
{}^0\hat{f}_{1z} &= {}^0f_{1z} - {}^0f_{2z} - mg = -0.012 && (39)\\
{}^0\hat{f}_{2y} &= {}^0f_{2y} + f_t = -0.027 && (40)\\
{}^0\hat{f}_{2z} &= {}^0f_{2z} + f_n - mg = -0.012 && (41)
\end{aligned}
$$

the result of above will be obtained. So, the translational acceleration of the center of mass of link 1 and link 2 will turn to ${}^0\hat{\boldsymbol{f}}_1/m_1 = [0, -0.009, -0.012]^{\mathrm{T}}$, ${}^0\hat{\boldsymbol{f}}_2/m_2 = [0, -0.027, -0.012]^{\mathrm{T}}$, it is consistent with the value of Ⓐ${}^0\ddot{\boldsymbol{s}}_1$, ${}^0\ddot{\boldsymbol{s}}_2$ above.

Then when ② ($t = 4.85$), the force acting on each link and its acceleration can be obtained as ${}^0\boldsymbol{f}_1 = [0, -0.088, 10.074]^{\mathrm{T}}$, ${}^0\boldsymbol{f}_2 = [0, -0.090, 0.271]^{\mathrm{T}}$, $f_t = 0.095$, $f_n = 9.533$, ${}^0\ddot{\boldsymbol{s}}_1 = [0, 0.002, 0.003]^{\mathrm{T}}$, ${}^0\ddot{\boldsymbol{s}}_2 = [0, 0.006, 0.003]^{\mathrm{T}}$. Therefore, all external forces acting on each link at the time of $t = 4.85$ in the same manner as in Eq.(38)∼Eq.(41) is ${}^0\hat{\boldsymbol{f}}_1 = [0, 0.002, 0.003]^{\mathrm{T}}$, ${}^0\hat{\boldsymbol{f}}_2 = [0, 0.006, 0.003]^{\mathrm{T}}$. And translational acceleration of the center of mass of link 1 and link 2 will become ${}^0\hat{\boldsymbol{f}}_1/m_1 = [0, 0.002, 0.003]^{\mathrm{T}}$, ${}^0\hat{\boldsymbol{f}}_2/m_2 = [0, 0.006, 0.003]^{\mathrm{T}}$, there is no contradiction between the relationship of acting force and acceleration at the time of ② similar to time of ①.

Then, we examined the acting force and constraint force acting between each link of 3-link manipulator. We set the posture ($\boldsymbol{q} = [-0.05, -\pi/2 + 0.05, -\pi/2 + 0.05]^{\mathrm{T}}$) in Fig.12(a) that was displaced by 0.05 angle from the balance point of $\boldsymbol{q} = [0, -\pi/2, -\pi/2]^{\mathrm{T}}$ as the initial posture, finally, we made the free response simulation that converge to balance point of Fig.12(b). Here, Fig.13 shows screen shot of simulation and Fig.14 shows the time response of the y-component of the force ${}^0\boldsymbol{f}_1 = [{}^0f_{1x}, {}^0f_{1y}, {}^0f_{1z}]^{\mathrm{T}}$, ${}^0\boldsymbol{f}_2 = [{}^0f_{2x}, {}^0f_{2y}, {}^0f_{2z}]^{\mathrm{T}}$, ${}^0\boldsymbol{f}_3 = [{}^0f_{3x}, {}^0f_{3y}, {}^0f_{3z}]^{\mathrm{T}}$, acting on each joint and the frictional force f_t acting on hand. Fig.15 shows the time response of the z-component and constraint force f_n,and Table 3 shows the physical parameters, besides Table 4 shows the initial value and final value. In Fig.14 and 15, we set the time of $t = 3.01$ as ③ and the time of $t = 3.95$ as ④. For ③, ④, Fig.16 shows the direction of acceleration and the force acting on direction y, z. In the case of ③ ($t = 3.01$), the force and acceleration will become ${}^0\boldsymbol{f}_1 = [0, 0.368, 16.952]^{\mathrm{T}}$, ${}^0\boldsymbol{f}_2 = [0, 0.308, 7.322]^{\mathrm{T}}$, ${}^0\boldsymbol{f}_3 = [0, 0.197, -2.134]^{\mathrm{T}}$, $f_t = -0.118$, $f_n = 11.760$, ${}^0\ddot{\boldsymbol{s}}_1 = [0, 0.060, -0.170]^{\mathrm{T}}$, ${}^0\ddot{\boldsymbol{s}}_2 = [0, 0.111, -0.343]^{\mathrm{T}}$, ${}^0\ddot{\boldsymbol{s}}_3 = [0, 0.079, -0.174]^{\mathrm{T}}$, we can calculate all external forces acting on each link in the same manner in Eq.(38)∼(41) at the time of $t = 3.01$ are ${}^0\hat{\boldsymbol{f}}_1 = [0, 0.060, -0.170]^{\mathrm{T}}$, ${}^0\hat{\boldsymbol{f}}_2 = [0, 0.111, -0.343]^{\mathrm{T}}$ and ${}^0\hat{\boldsymbol{f}}_3 = [0, 0.079, -0.174]^{\mathrm{T}}$. Therefore we got the same value of the acceleration obtained from ${}^0\hat{\boldsymbol{f}}_i/m_i$, so there is no contradiction between the relationship of acting force and acceleration.

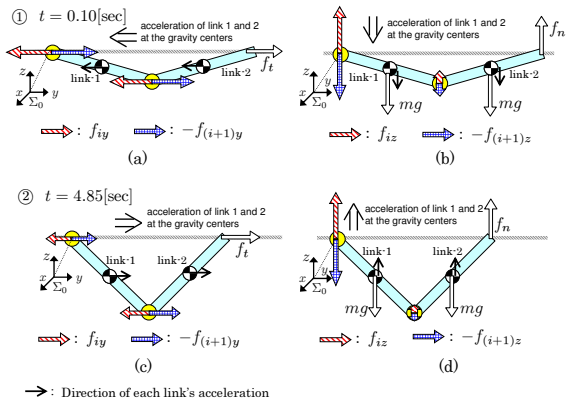

Fig. 11. Forces acting on each link and accelerations of each link at ① $t = 0.10$ [sec] are shown at (a) as for y-direction and (b) as for z-direction. Also, at ② $t = 4.85$ [sec] they are shown at (c) as for y-direction and (d) as for z-direction.

In the case of ④ ($t = 3.95$), the force and acceleration will become ${}^0\boldsymbol{f}_1 = [0, -1.772, 16.826]^{\mathrm{T}}$, ${}^0\boldsymbol{f}_2 = [0, -1.499, 7.033]^{\mathrm{T}}$, ${}^0\boldsymbol{f}_3 = [0, -0.968, -2.803]^{\mathrm{T}}$, $f_t = -0.127$, $f_n = 12.658$, ${}^0\ddot{\boldsymbol{s}}_1 = [0, -0.274, -0.007]^{\mathrm{T}}$, ${}^0\ddot{\boldsymbol{s}}_2 = [0, -0.007, -0.036]^{\mathrm{T}}$, ${}^0\ddot{\boldsymbol{s}}_3 = [0, -0.841, -0.055]^{\mathrm{T}}$. All external forces acting on each link at the time of $t = 3.95$ are ${}^0\hat{\boldsymbol{f}}_1 = [0, -0.274, -0.007]^{\mathrm{T}}$, ${}^0\hat{\boldsymbol{f}}_2 = [0, -0.007, -0.036]^{\mathrm{T}}$, ${}^0\hat{\boldsymbol{f}}_3 = [0, -0.841, -0.055]^{\mathrm{T}}$. Therefore we got the same value of the acceleration obtained from ${}^0\hat{\boldsymbol{f}}_i/m_i$, so there is no contradiction between the relationship of acting force and acceleration. And Fig.14 shows the acting force in y-direction is maximum in the negative direction at the time of ④. We can know that the shape of manipulator in this case has a shape close to a specific shape as shown in Fig.13 and Fig.16(c), (d). It shows that the force acting on each link will increase at the specific shape nearby.

VI. CONCLUSION

In this paper, we proposed the iterative calculation method to represent the constraint motion by using inverse dynamics calculation of the Newton-Euler method, and we have shown a solving method of the forward dynamics calculation. The results of simulation show the hand restraint motion of manipulator can be expressed by proposed calculation method, and it is possible to calculate the force acting on each link.

As remaining tasks in the future, we will extend the calculation method to the case of multi-point restraint situations,

that has more than two constraint conditions, and we will evaluate it by numerical simulations.

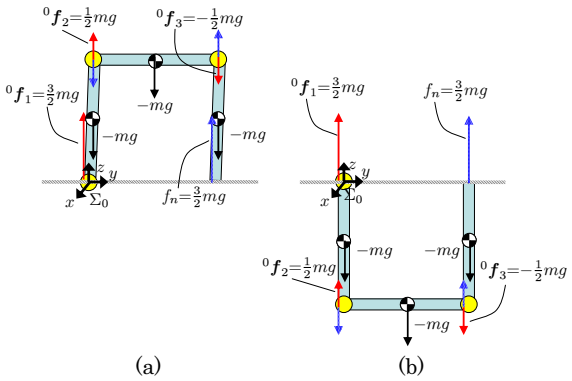

Fig. 12. Initial angle of 3-link manipulator is set to $\boldsymbol{q} = [-0.05, -\pi/2 + 0.05, -\pi/2 + 0.05]^{\mathrm{T}}$ as (a). As a result of free response($\boldsymbol{\tau} = \boldsymbol{0}$), manipulator converged at $\boldsymbol{q} = [-\pi, \pi/2,]^{\mathrm{T}}$ as (b).

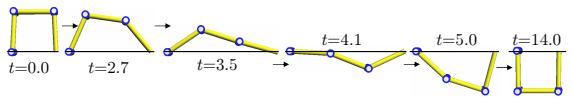

Fig. 13. Screen shot of free response of 3-link manipulator

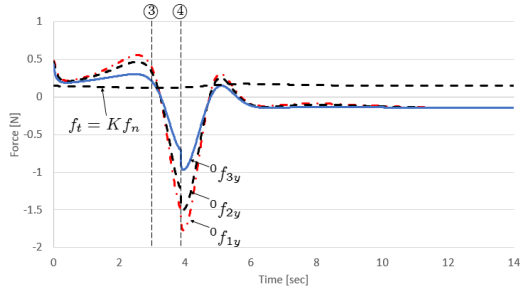

Fig. 14. Time response of y component of forces acting on each link ${}^0f_{1y}$, ${}^0f_{2y}$, ${}^0f_{3y}$ and frictional force f_t of 3-link manipulator are plotted.$f = Kf_n$, $K = 0.01$

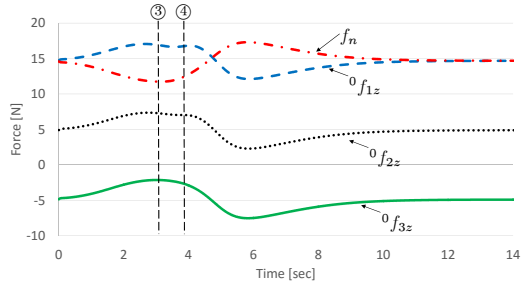

Fig. 15. Time response of z component of forces acting on each link ${}^0f_{1z}$, ${}^0f_{2z}$, ${}^0f_{3z}$ and normal force f_n of 3-link manipulator are plotted.

REFERENCES

[1] Brady, M., Hollerbach, J. M., Johnson, T. L., Lozano-Perez, T. and Mason, M. T., Robot motion: planning and control (1982), pp. 51-71, The MIT Press.

TABLE III

PHYSICAL PARAMETERS OF 3-LINK MANIPULATOR

Link number i	1 (i=1)	2 (i=2)	3 (i=3)
m_i [kg]	1.0	1.0	1.0
l_i [m]	0.5	0.5	0.5
D_i [N · m · s/rad]	3.0	3.0	3.0
τ_i [N · m]	0	0	0
g [m/s^2]	9.8		
K	0.01		

TABLE IV

INITIAL AND CONVERGED VALUES OF $q_1, q_2, q_3, {}^0f_1, {}^0f_2, {}^0f_3, {}^0f_n$

Link number i	1 (i=1)	2 (i=2)	3 (i=3)
Initial angle q_i [rad]	-0.05	$-\pi/2+0.05$	$-\pi/2+0.05$
Converged value of q_i [rad]	$-\pi$	$\pi/2$	$\pi/2$
Converged value of ${}^0\boldsymbol{f}_i$ [N]	$[0, -0.147, 14.7]^{\mathrm{T}}$	$[0, -0.147, 4.9]^{\mathrm{T}}$	$[0, -0.147, -4.9]^{\mathrm{T}}$
Converged value of ${}^0f_n$ [N]	14.7		

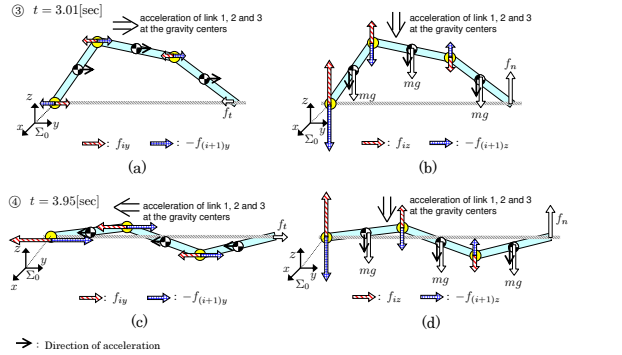

Fig. 16. Forces acting on each link and accelerations of each link at ③ $t = 3.01$ [sec] are shown at (a) as for y-direction and (b) as for z-direction. Also, at ④ $t = 3.95$ [sec] they are shown at (c) as for y-direction and (d) as for z-direction.

[2] Hooker, W.W., Margulies, G., The Dynamical Attitude Equations for an n-body Satellite, Journal of Astronautical Sciences, Vol. 12 (1965), pp. 123-128.

[3] Stepanenko, Y. and Vukobratovic, M., Dynamics of Articulated Open-chain Active Mechanisms', Mathematical Biosciences, Vol. 28, Iss. 1-2 (1976), pp. 137-170.

[4] Walker, M. W. and Orin, D. E., Efficient Dynamic Computer Simulation of Robotic Mechanisms, Transactions of ASME, Journal of Dynamic Systems, Measurement, and Control, Vol. 104, No. 3 (1982), pp. 205-211.

[5] Huang, Y. F. and Lee, C. S. G., Generalization of Newton-Euler Formulation of Dynamic Equations to Nonrigid Manipulators, Transactions of ASME, Journal of Dynamic Systems, Measurement, and Control, Vol. 110, No. 3 (1988), pp. 308-315.

[6] Hasegawa S., Mitrake H. and Tazaki Y., Springhead: A Physics Engine for Motion and Behavior, Journal of RSJ, Vol. 30, No. 9 (2012), pp.841-848 (in Japanese).

[7] Anitescu M. and Potra A. F., A time-stepping method for stiff multibody dynamics with contact and friction, International Journal for Numerical Methods in Engineering, Vol. 55 (2002), pp. 753-784.

[8] Featherstone. R. and Orin. D., Robot Dynamics: Equations and Algorithms, IEEE International Conference on Robotics and Automation (2000), pp. 826-834.

[9] Nakamura, Y. and Yamane, K., Dynamics of Kinematic Chains with Discontinuous Changes of Constraints—Application to Human Figures that Move in Contact with the Environments—, Journal of RSJ, Vol.18, No.3 (2000), pp.435–443 (in Japanese).

[10] Hemami, H. and Wyman, B. F., Modeling and control of constrained dynamic systems with application to biped locomotion in the frontal plane, IEEE Transactions on Automatic Control, Vol. AC-24, No, 4 (1979), pp. 526-535.